Expression of Developmentally Important Axon Guidance Cues in the Adult Optic Chiasm

Raquel Conceição,[1] Rachel S. Evans,[1] Craig S. Pearson,[1,2] Barbara Hänzi,[1] Andrew Osborne,[1] Sarita S. Deshpande,[1] Keith R. Martin,[1,3–5] and Amanda C. Barber[1]

[1]John van Geest Centre for Brain Repair, Department of Clinical Neurosciences, University of Cambridge, United Kingdom
[2]Laboratory of Developmental Neurobiology, National Heart, Lung, and Blood Institute, National Institutes of Health, Bethesda, United States
[3]Centre for Eye Research Australia, Melbourne, Australia
[4]University of Melbourne, Melbourne, Australia
[5]Department of Ophthalmology, NIHR Biomedical Research Centre and Wellcome Trust-MRC Cambridge Stem Cell Institute, University of Cambridge, United Kingdom

Correspondence: Keith R. Martin, John van Geest Centre for Brain Repair, Department of Clinical Neurosciences, University of Cambridge, CB2 0PY, United Kingdom; krgm2@cam.ac.uk.

Submitted: January 25, 2019
Accepted: August 21, 2019

Citation: Conceição R, Evans RS, Pearson CS, et al. Expression of developmentally important axon guidance cues in the adult optic chiasm. *Invest Ophthalmol Vis Sci*. 2019;60:4727–4739. https://doi.org/10.1167/iovs.19-26732

Purpose. Regeneration of optic nerve axons after injury can be facilitated by several approaches, but misguidance at the optic chiasm is often observed. We characterized guidance cues in the embryonic visual system and adult optic chiasm before and after optic nerve crush (ONC) injury to better understand barriers to optic nerve regeneration in adults.

Methods. Radial glial (RC2/BLBP/Slit1), developmental (Pax2) and extracellular markers (CSPG: H2B/CS-56) were assessed in C57BL/6J mice by immunohistochemistry. RC2, BLBP, Slit1, and CSPG are known inhibitory guidance cues while Pax2 is a permissive guidance cue.

Results. At embryonic day 15.5 (E.15.5), RC2 and BLBP were identified superior to, and extending through, the optic chiasm. The optic chiasm was $BLBP^{-ve}$ in adult uninjured mice but $BLBP^{+ve}$ in adult mice 10 days after ONC injury. The reverse was true for RC2. Both BLBP and RC2 were absent in adult mice 6 weeks post-ONC. Slit1 was present in the optic chiasm midline and optic tracts in embryonic samples but was absent in uninjured adult tissue. Slit1 was observed superior to and at the midline of the optic chiasm 10 days post-ONC but absent 6 weeks after injury. Pax2 was expressed at the junction between the optic nerve and optic chiasm in embryonic brain tissue. In embryonic sections, CS-56 was observed at the junction between the optic chiasm and optic tract, and immediately superior to the optic chiasm. Both 2H6 and CS-56 staining was absent in uninjured and ONC-injured adult brains.

Conclusion. Differences in guidance cue expression during development, in adulthood and after injury may contribute to misguidance of regenerating RGC axons in the adult optic chiasm.

Keywords: optic chiasm guidance cues

The optic chiasm is a midline structure of the visual system located behind the hypothalamus, where retinal ganglion cell (RGC) axons from both optic nerves converge before exiting to either the ipsilateral or contralateral optic tract. Achieving robust optic nerve regeneration beyond the optic chiasm after optic nerve injury has proven challenging.[1–14] In recent years, several authors claim to have achieved long distance axonal regeneration beyond the optic chiasm with some evidence of function recovery.[4,8–11,13] However, these same papers describe axonal misguidance and misrouting errors at the optic chiasm, including frequent U-turns and sometimes misguidance into the contralateral optic nerve. Interestingly, the pathfinding errors of regenerating RGC axons are phenotypically similar to errors documented in RGC axon development when key guidance cues are absent or ectopically expressed.[15]

In the developing embryo, there are a number of guidance cues that are expressed in the brain in a highly organized spatial and temporal fashion to ensure that developing RGC axons project correctly through the optic chiasm and toward their central targets. Axon-guidance molecules include neutrins, semaphorins, laminin, multiple members of the Ephrin/Eph families, glial markers, slits, and chondroitin sulfate proteoglycan molecules.[16–38] Pair box–containing gene, Pax2, is an essential guidance cue during embryogenesis and is expressed by astroglia in the optic nerve throughout development to form a growth promoting corridor to guide newly developing RGC axons along the optic nerve towards the developing optic chiasm.[16,39–43]

The glial markers radial glial cell marker 2 (RC2), brain lipid binding protein (BLBP) and slit guidance ligand 1 (Slit1) have been identified in the area surrounding the embryonic optic chiasm and are usually described as inhibitory guidance cues. It is believed these inhibitors assist in directing newly formed RGC axons towards the optic tracts in both sides of the brain, thus avoiding misguidance into surrounding tissue.[16,18,19–21,23,27,33–36,44–46] Slit1 in particular restricts RGC axons extending outside the optic chiasm whilst BLBP and RC2 positive radial glia, located immediately posterior to the murine

optic chiasm,[20,32,46,47] possess short end-feet projections that interact with and guide retinal axons through the chiasm.

The boundary-forming inhibitory properties of chondroitin sulfate proteoglycans (CSPGs) are critical for axon guidance at the optic chiasm and these are mediated by their sulfated glycosaminoglycan (GAG) chains. In the current study, we used 2 antibodies against CSPGs: the CS-56 antibody reacts with 4S (4-sulfated) and 6S (6-sulfated) groups of the GAG chains and the 2H6 antibody reacts predominantly with 4S groups.[48] When RGC axons first enter the chiasm (E13–E14), CSPG levels are low in the optic fiber layer but robust in the caudal parts of the ventral diencephalon.[37] Where axons cross the midline toward the optic tract, CSPGs have been observed at the site where ventral axons are sorted from dorsal axons.[37] Removal of GAG chains from embryo brains by intraventricular injection of chondroitinase ABC (ChABC) led to an enlargement of the anterior optic tract, suggesting that CSPGs define the optic tract's anterior boundary.[49] Studies using ChABC indicate that CSPGs may also be essential for establishing age-related axonal organization in the mouse optic tract.[50] Overall, the positioning of CSPGs act to inhibit axons and form distinct boundaries during optic chiasm development.

In order to understand why optic nerve regeneration through the optic chiasm is so challenging, a deeper understanding of the adult extracellular optic chiasm environment is needed. Currently, it is unknown whether the guidance cues that are essential for correct axon pathfinding during embryogenesis are retained in the adult optic chiasm. This study therefore aims to characterize the expression of the key guidance cues RC2, BLBP, Slit1, Pax2, and CSPGs at the optic chiasm region of embryonic (E15.5), adult and adult ONC-injured mice.

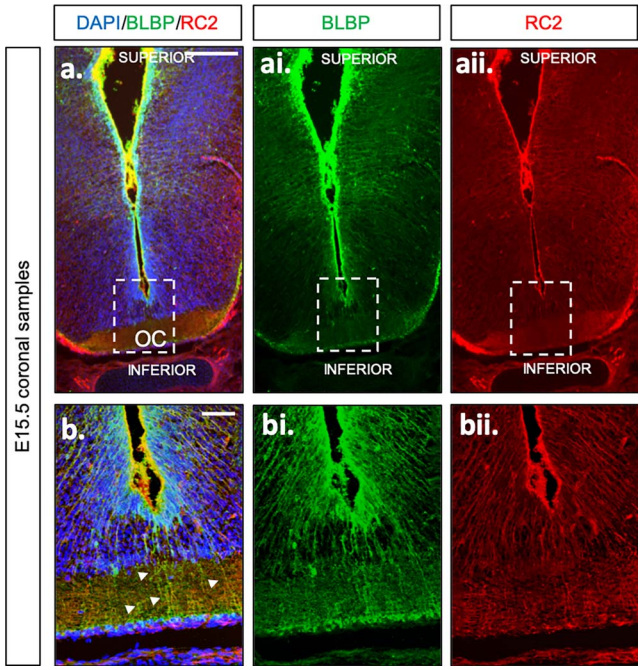

Figure 1. RC2 (*red*) and BLBP (*green*) staining of E15.5 mouse coronal samples. (**a–aii**) Images of the OC and surrounding structures. *Scale bar*: 500 µm. (**b–bii**) High-power images show the chiasm structure in detail. (**ai**) BLBP and (**aii**) RC2 positive staining was observed immediately superior to the optic chiasm and glial processes (*arrows,* **b**) can be observed interacting with the optic chiasm. *Blue*: DAPI. *Scale bar*: 100 µm.

Methods

In Vivo Work

All in vivo work was carried out in accordance with the UK Home Office Regulations for the Care and Use of Laboratory Animals, the 1986 UK Animals (Scientific Procedures) Act , and the ARVO Statement for the Use of Animals in Ophthalmic and Visual Research. Embryos were collected at E11.5 ($n = 4$) and E15.5 ($n = 4$) via cesarean section from pregnant C57BL/6J mice. Embryos were decapitated and brains were fixed in 4% paraformaldehyde (PFA) at 4°C overnight. Adult C57BL/6J mice aged 6 to 8 weeks were culled uninjured ($n = 8$) or received an optic nerve crush ($n = 8$/timepoint) as previously described.[5] Briefly, the optic nerve was exposed intraorbitally by cutting the conjunctival membrane and the nerve was crushed approximately 1 mm behind the eye for 10 seconds. Injury was validated 10 days and 6 weeks post optic nerve crush (pONC) by immunohistochemistry and quantification of surviving RGCs from retinal whole-mounts (Supplementary Fig. S1). Mice were perfused with 4% PFA prior to tissue collection.

Brain Histology

Fixed brain tissue was cryopreserved in 30% sucrose at 4°C overnight and embedded in water-soluble glycols and resins (Tissue-Tek O.C.T. Compound, 25608-930, Sakura Finetek Europe B.V., AJ Alphen aan den Rijn, The Netherlands) for the production of coronal sections (14-µm thick) using a cryostat (Leica Microsystems, Wetzlar, Germany). For RC2, BLBP, Slit1 and Pax2 immunohistochemistry, brain sections were blocked with 3% BSA, 10% normal goat serum (NGS) in 0.1% PBS-Triton X-100. Radial glial markers: RC2 (mouse, 1:5; Developmental Studies Hybridoma Bank), BLBP (rabbit, 1:500, ab32423; Abcam, Cambridge, UK), Slit1 (rabbit, 1:500, PAB11326; AbNova, Taipei, Taiwan) and embryonic development marker Pax2 (rabbit, 1:100, 901001; BioLegend, San Diego, CA, USA) were diluted in blocking solution at 4°C overnight. For CS-56 and H2B immunohistochemistry, brain sections were blocked with 3% NGS in 0.2% PBS-Triton X-100. CSPG markers: CS-56 (mouse, 1:500, C8035; Sigma-Aldrich Corp., St. Louis, MO, USA) and H2B (mouse, 1:500, 370710-IEC; Amsbio, Madrid, Spain) were also diluted in blocking solution and incubated at 4°C overnight. Where the primary antibody was raised in mouse, a mouse on mouse Ig blocking solution (BMK-2202; Vector Laboratories, Burlingame, CA, USA) was applied to avoid nonspecific staining. For each set of immunostaining, a no primary antibody control was included to ensure staining was specific (Supplementary Figs. S2, S3). For the CSPG, crushed optic nerve samples were also analyzed to visualize the injury site (Supplementary Fig. S4). For GFAP, NG2, Iba1, and Olig2 immunohistochemistry, brain sections were blocked with 2% BSA, 5% NGS in 0.5% PBS-Triton X-100. GFAP (chicken, 1:1000, ab4674; Abcam), NG2 (rabbit, 1:200, AB5320; MilliporeSigma, Burlington, MA, USA), Iba1 (guinea pig, 1:500, #234004/6; Synaptic Systems, Göttingen, Germany) and Olig2 (rabbit, 1:500, AB9610, MilliporeSigma) were diluted in blocking solution at 4°C overnight. Slides were washed three times for 10 minutes with PBS. Anti-rabbit Alexa Fluor-555 (1:500, A-21429; Invitrogen, Carlsbad, CA, USA), anti-mouse Alexa Fluor-555 (1:500, A21424; Invitrogen), anti-rabbit Alexa Fluor-488 (1:500, A11034; Invitrogen), anti-chicken Alexa Fluor-488 (1:500, A11039; Invitrogen), anti-rabbit Alexa Fluor-647 (1:500, A32733; Invitrogen), anti-mouse Alexa Fluor-488 (1:500, A11029; Invitrogen), anti-guinea pig Alexa Fluor-555 (1:500, A21435; Invitrogen) and anti-guinea pig Alexa Fluor-488

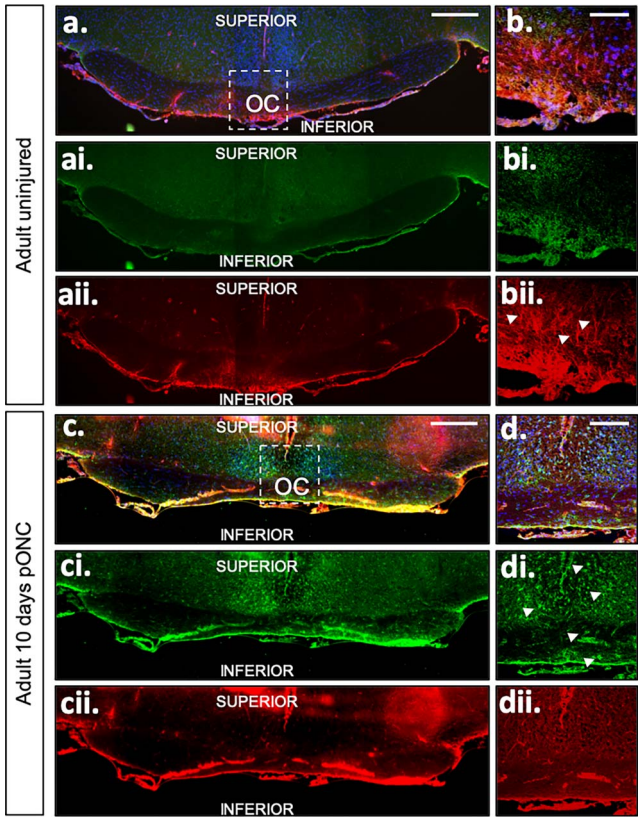

Figure 2. RC2 (*red*) and BLBP (*green*) staining of adult uninjured and 10 days pONC mouse coronal samples. Images of the OC and surrounding structures are shown and in (**a–aii**) adult-uninjured and (**c–cii**) -injured samples. *Scale bar*: 500 µm. High-power images of (**b–bii**) adult-uninjured and (**d–dii**) -injured samples show the chiasm structure in detail. *Blue*: DAPI. *Scale bar*: 100 µm. RC2-positive and BLBP-negative processes were observed extending through the optic chiasm midline (*arrows,* **bii**) in uninjured adult mice; while in 10-day pONC adult mice, only BLBP-positive staining was observed (*arrows,* **di**).

(1:500, A11073; Invitrogen) were used as secondary antibody with a 2-hour incubation period at room temperature, followed by counterstaining with DAPI. Slides were washed three times for 10 minutes with PBS and mounted with glass coverslips and reagent (FluorSave, 345789; MilliporeSigma).

Retinal Histology

For RGC quantification, eyes were collected, and the retinas extracted and flattened into whole-mounts. Retinas were fixed in 4% PFA for 2 hours and washed four times with 0.5% PBS-Triton X-100. In between the second and third wash, a permeation step was performed to improve antibody penetration by freezing the retinas in 0.5% PBS-Triton X-100 for 10 minutes at −70°C, and washing was continued after thawing. Retinal whole-mounts were blocked with 2% BSA, 10% donkey serum in 2% PBS-Triton X-100. Brn3A (C-20, goat, 1:200, sc-31984; Santa Cruz Biotechnology, Dallas, TX, USA) was diluted in blocking solution for 2 hours incubation at room temperature and then at 4°C overnight. Anti-goat Alexa Fluor-555 (1:500, A32816; Invitrogen) was used as secondary antibody in 2% PBS-Triton X-100 with a 2 hours incubation period at room temperature, followed by counterstaining with DAPI. After this, three wash steps with PBS were performed. Finally, retinal whole-mounts were mounted onto slides with reagent (345789, MilliporeSigma) and stored at 4°C until imaging.

Microscopy/Cell Quantification

Immunofluorescence was analyzed using epifluorescence and confocal microscopy (Leica CTR 6000, Leica DMI 4000B; Leica Microsystems). For the retinal whole-mounts, eight images (4 central, 4 peripheral) were analyzed at ×20 magnification as previously described.[51] Images were analyzed in ImageJ Fiji (Fiji-win64, http://imagej.nih.gov/ij/; provided in the public domain by the National Institutes of Health, Bethesda, MD, USA) using the ICTN Plugin to count Brn3A-positive cells with the following settings: width = 22, minimum distance = 5, and threshold = 0.1. Eight images represent approximately 21% of the total retinal surface area so the total number of RGCs was estimated for each retina multiplying the sum from these eight images by 4.7. Survival pONC was expressed as a percentage of the uninjured contralateral right eye.

For the optic chiasm, images were taken at ×40 magnification using confocal microscopy. For each image, the optic chiasm region was outlined in ImageJ Fiji (Fiji-win64) and the area was calculated in mm^2 using the scale bar for calibration. DAPI-positive cells within this region were counted manually and divided by the total area to give a value in cells/mm^2. To quantify NG2, GFAP, Iba1, and Olig2, the number of DAPI-positive cells colocalized to each marker was counted manually and expressed as a percentage of the total number of DAPI-positive cells. A minimum of 3 brain sections was counted per

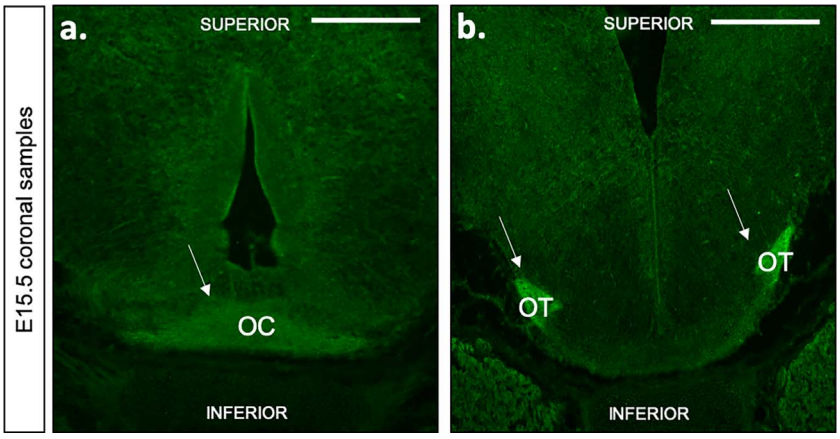

Figure 3. Slit1 (*green*) staining of embryonic day E15.5 mouse coronal samples. Images of the embryonic OC, OT, and respective surrounding structures are shown in (**a**, **b**), respectively. Slit1 positive staining was observed in the optic chiasm midline (*arrow,* **a**) and also in more posterior sections where the optic tract is visible (*arrows,* **b**). *Scale bar*: 500 µm.

Investigative Ophthalmology & Visual Science

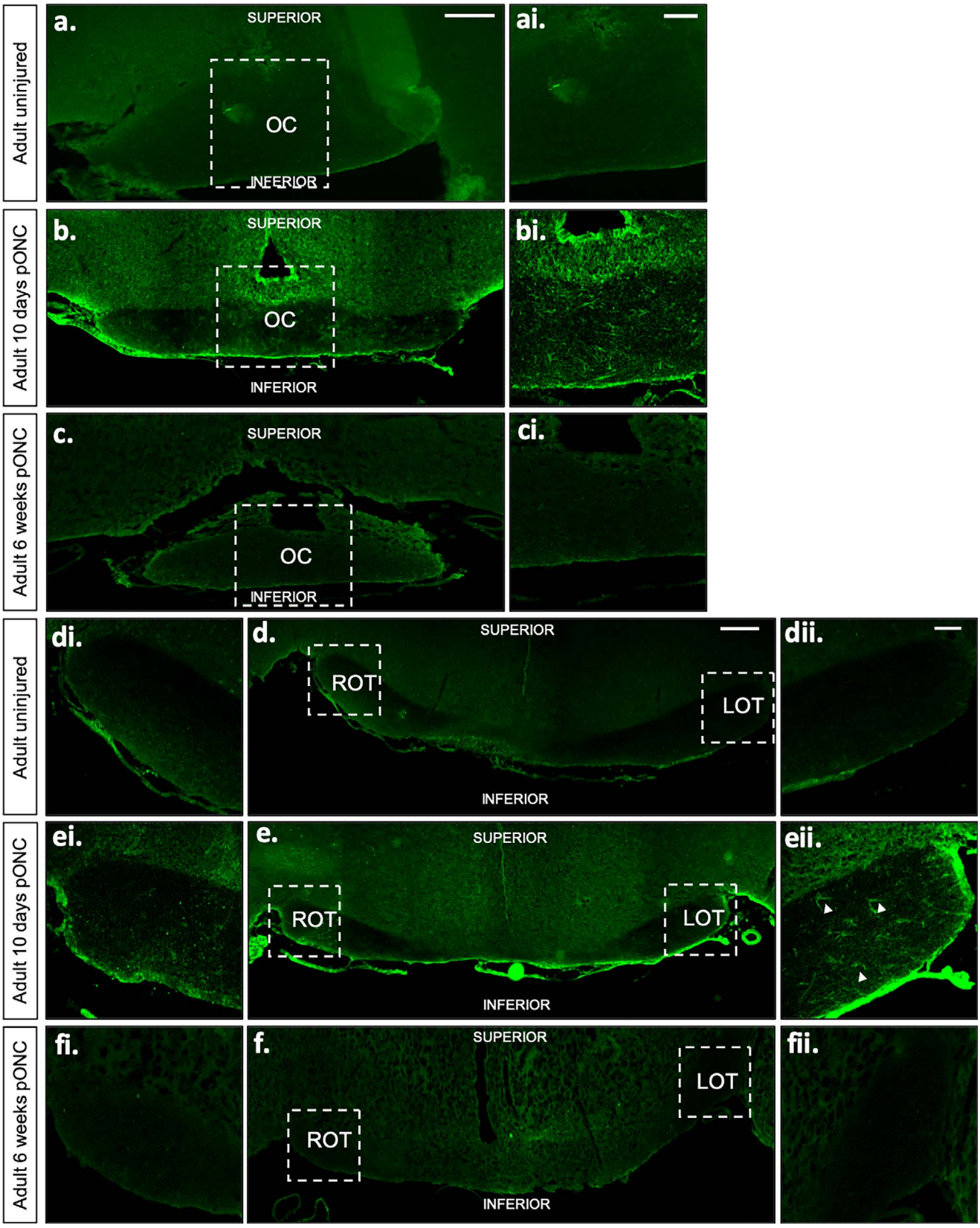

Figure 4. Slit1 (*green*) staining of adult uninjured and injured mouse in coronal samples. Images of the OC, OT, and surrounding structures in adult-uninjured samples are shown in (**a**, **d**); adult samples 10 days pONC are shown in (**b**, **e**); and adult samples 6 weeks pONC are shown in (**c**, **f**). *Scale bar*: 500 μm. High-power images of each *dotted area* are shown. *Scale bar*: 100 μm. Slit1-positive staining was observed at the optic chiasm midline and immediately above it 10 days pONC (**b**–**bi**), but the same was not observed in uninjured adult samples (**a**–**ai**) and 6-week pONC samples (**c**–**ci**). Interestingly, also at 10 days pONC, slit1-positive staining was present only in the right optic tract and this pattern was not observed in the other two conditions.

Investigative Ophthalmology & Visual Science

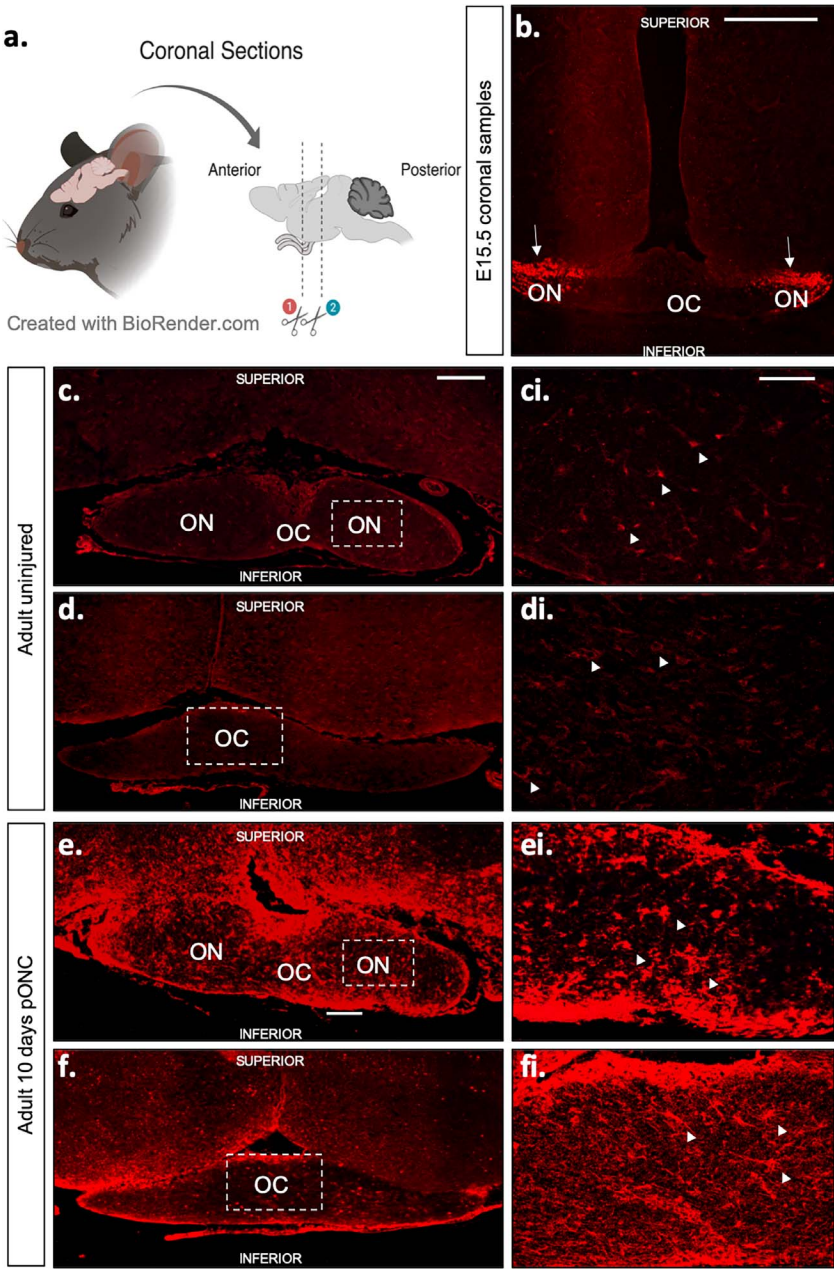

Figure 5. Pax2 (*red*) staining of E15.5, adult uninjured and adult 10-day pONC mouse coronal samples. Mouse brains were collected and sections were collected following a coronal orientation (**a**); images of the OC, optic nerve ON, and surrounding structures are shown in (**b**–**f**). Positive Pax2 staining is indicated by the arrows. Pax2 positive staining was observed at the junction between the optic nerves and chiasm in embryonic E15.5 samples (**b**); while in adult uninjured (**c**, **d**) and 10-day pONC (**e**, **f**) brain samples, positive Pax2 staining was observed evenly dispersed throughout the optic chiasm. *Scale bar*: 500 µm. Higher magnification images of the optic chiasm midline for both uninjured and 10-day pONC are presented in (**ci**–**di**, **ei**–**fi**), respectively. *White arrows* indicate positive staining. *Scale bar*: 100 µm.

animal using 3 mice per group: embryonic, adult uninjured, adult injured (10 days pONC) and adult injured (6 weeks pONC).

Results

RC2/BLBP

RC2 and BLBP are glial markers that create an inhibitory region for developing RGC axons. Staining for glial markers RC2 (red) & BLBP (green) was detected immediately superior to the optic chiasm in coronal E15.5 samples, as can be observed in Figure 1 and the accompanying higher magnification images (Fig. 1b, as indicated by the dotted box). In E15.5 samples, radial glial cell processes positive for both BLBP and RC2 can be observed crossing the optic chiasm (Fig. 1b, arrows).

In coronal uninjured adult brain samples, RC2- positive processes were observed extending through the optic chiasm midline (Fig. 2bii, arrows). Processes were negative for BLBP, contrary to what was observed in the embryonic samples. In addition, RC2 and BLBP staining superior to the optic chiasm was absent in uninjured adult samples contrary to that in the

Investigative Ophthalmology & Visual Science

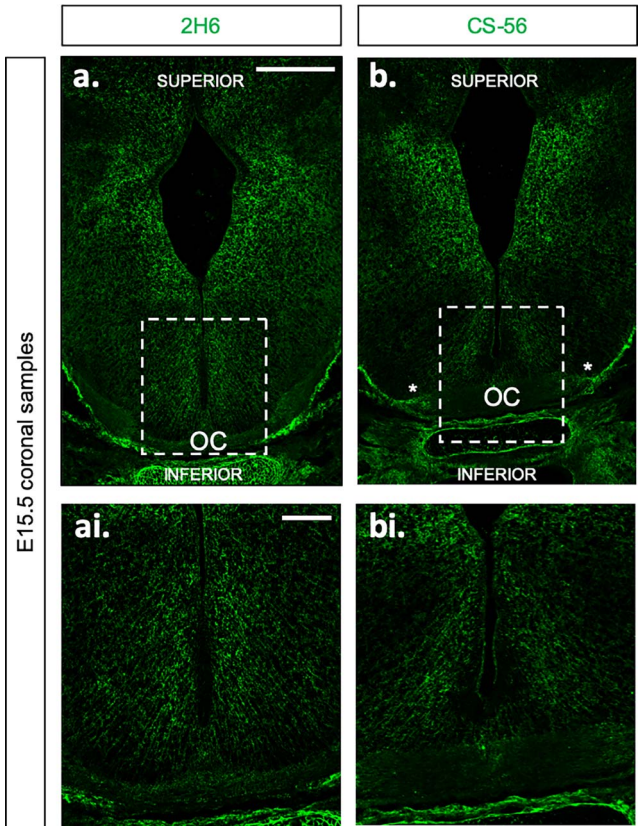

Figure 6. CSPG (*green*) staining of embryonic day E15.5 mouse coronal samples. Images of the OC and surrounding structures are shown. (**a**) Shows 2H6 staining and (**b**) shows CS-56 staining. *Scale bar*: 500 µm. High power images in panel ai and bi show the chiasm structure in detail. *Scale bar*: 100 µm. Both 2H6 and CS-56 staining were detected immediately above the optic chiasm (**a–ai**, **b–bi**, respectively) and CS-56 was also detected at the connection between optic nerves and optic chiasm (*stars*, **b**).

embryonic samples (Fig. 1). In coronal sections obtained from 10 days pONC adult mice, no RC2 or BLBP processes were observed in the optic chiasm midline (Figs. 2c, 2d), instead an activated BLBP+ glia morphology, characterized by hypertrophy of cellular processes, was observed both within the optic chiasm and in the region superior to the optic chiasm (Fig. 2di, arrows). In samples collected from adult mice 6 weeks pONC, no RC2 or BLBP staining was observed in any of the locations described previously (Supplementary Fig. S5a).

SLIT1

Slit1, which inhibits growth of developing RGCs axons, showed expression in the optic chiasm midline and optic tract at E15.5 (Fig. 3, green). No Slit1 staining was detected in the optic chiasm midline in brain samples obtained from uninjured adult mice (Figs. 4a, 4ai) and 6 weeks pONC adult mice (Figs. 4c, 4ci). However, positive Slit1 staining was observed in 10 days pONC adult mice, at the optic chiasm midline and the region immediately superior to the optic chiasm (Figs. 4b, 4bi). Slit1 staining was absent in adult uninjured optic tract sections shown in Figure 4d. Interestingly, Slit1 staining was observed in the right optic tract of adult mice 10 days after receiving ONC to the left nerve (Fig. 4eii, white arrows) but the same was not observed 6 weeks after injury (Fig. 4f).

Pax2

Pax2 is a developmental guidance cue expressed by astroglia and positively guides RGC axons through the optic nerve to the brain. Immunohistochemical analysis of Pax2 staining revealed positive expression at the junction between the optic nerves and chiasm in embryonic E15.5 samples (Fig. 5b, red). Additional E11.5 samples were analyzed to confirm expression of Pax2 in accordance with the current literature: Pax2 created a corridor beginning at the optic nerve head and continuing toward the ventral diencephalon, where the future optic chiasm is formed (Supplementary Fig. S6ai, red, arrows). Figure 5 demonstrates positive Pax2 staining evenly dispersed throughout the optic chiasm in adult uninjured (Figs. 5c, 5d) and 10 days pONC (Figs. 5e, 5f) brain samples. Pax2 staining was also observed at the junction between the optic nerves and optic chiasm in adult samples and which appeared upregulated in ONC samples compared to uninjured tissue (Figs. 5c–f). On the other hand, samples from 6 weeks pONC brains seemed to be absent of Pax2-positive staining (Supplementary Fig. S5b).

CSPGs

CSPGs are involved in axon guidance at the optic chiasm and act by inhibiting axonal growth in order to define boundaries. To detect the pattern of CSPG expression, two antibodies were used: CS-56, which reacts with the 4S and 6S groups on the glycosaminoglycan (GAG) portion of CSPG, and 2H6, which reacts predominantly with the 4S groups of CSPG. In E15.5 samples, positive staining for CS-56 was demonstrated at the junction between the optic chiasm and optic tracts in accordance with the literature[52] (Fig. 6c, as indicated by white stars). The optic chiasm midline was devoid of staining for both CS-56 and 2H6 in embryonic tissue, however, both markers were present in the region immediately superior to the optic chiasm (Fig. 6). In both the adult uninjured and adult ONC injured samples (both 10 days and 6 weeks pONC), no 2H6 or CS-56 staining was observed in any of the regions analyzed (Fig. 7).

Optic Chiasm Cell Density

During the study, it was observed that there was an increase in the number of DAPI-positive cells within the optic chiasm. An average of 583 ± 170 cells/mm^2 ($n = 4$) were present in the optic chiasm region at embryonic stage E15.5 (Fig. 8a), with a significant 4.2-fold increase to 2422 ± 414 cells/mm^2 ($n = 4$) in adult mice ($P = 0.0002$; Fig. 8b). An even larger increase was seen after optic nerve crush injury with a 5.1-fold increase to 2962 ± 590 cells/mm^2 ($n = 8$) at 10 days pONC ($P < 0.0001$; Fig. 8c), and a 6.0-fold increase to 3516 ± 433 ($n = 3$) at 6 weeks pONC ($P < 0.0001$; Fig. 8d). In addition, there was a significant 1.5-fold increase between adult uninjured and adult 6 weeks pONC samples ($P = 0.0193$).

To determine the cell populations in the optic chiasm, embryonic, adult uninjured and adult injured brain sections were stained with an antibody against GFAP (green), an astrocytic marker, and an antibody against NG2 (red), an oligodendrocyte precursor cell marker (Fig. 9). Another set of slides was stained with an antibody against ionized calcium binding adaptor molecule 1 (Iba1; green), a microglia marker, and oligodendrocyte transcription factor 2 (Olig2; red), an oligodendrocyte marker (Fig. 10).There were very few DAPI-positive labelled cells in the optic chiasm at embryonic E15.5 (Fig. 8a), with no obvious GFAP, NG2, Iba1 or Olig2 immunoreactivity (Figs. 9ai–aiv, 10ai–aiv). However, positive

Investigative Ophthalmology & Visual Science

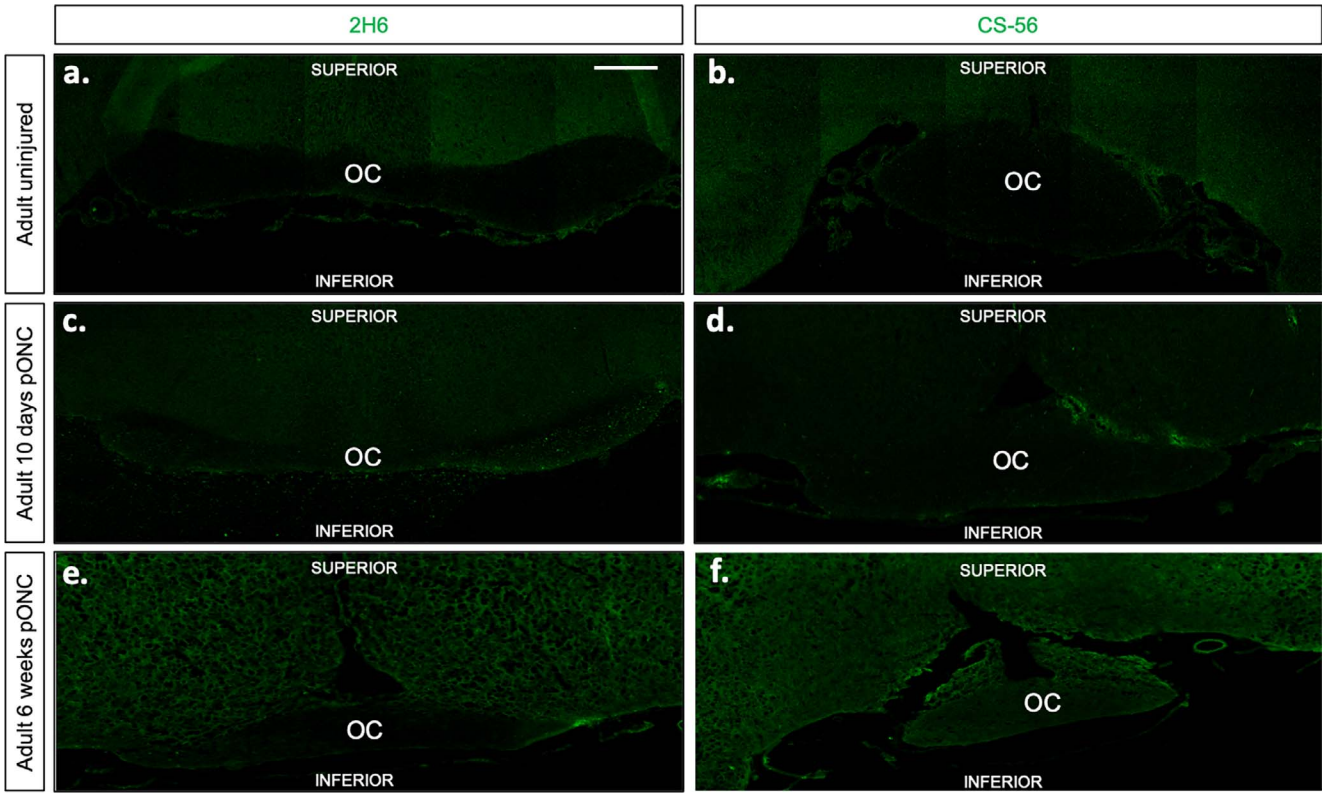

Figure 7. CSPG (*green*) staining of adult uninjured and injured mouse coronal samples. Images of the OC and surrounding structures are stained with 2H6 (**a**, **c**, **e**), and CS-56 (**b**, **d**, **f**). *Scale bar*: 500 µm. Both guidance cue markers were not detected in adult uninjured samples (**a**, **b**), in 10-day pONC samples (**c**, **d**) and in 6-week pONC samples (**e**, **f**).

staining for each marker was seen in the adult uninjured and injured samples.

As summarized in the graph (Fig. 9e), 12.9% ± 5.8% of cells were GFAP-positive in adult uninjured mice (Fig. 9bii), which increased slightly to 16.5% ± 9.0% in injured mice 10 days pONC (Fig. 9cii) and then decreased slightly to 6.0% ± 1.1% in injured mice 6 weeks pONC (Fig. 9dii). These changes were not statistically significant. A similar proportion of cells were NG2-positive in adult uninjured mice (10.7% ± 3.9%; Fig. 9biii), 10 days pONC (11.9% ± 4.3%; Fig. 9ciii) and 6 weeks pONC (4.9% ± 1.3%) with no significance between groups.

Significant changes were seen in Iba1 staining. As summarized in the graph (Fig. 10e), 3.3% ± 0.7% of cells were Iba1-positive in adult uninjured mice (Fig. 10bii), which significantly increased in injured mice to 8.2% ± 2.2% at 10 days pONC ($P = 0.0219$; Fig. 10cii) and to 11.9% ± 2.7% at 6 weeks pONC ($P = 0.0057$; Fig. 10dii). No difference was seen between the two injured groups. The majority of cells were Olig2-positive with 54.4% ± 10.2% of cells positive for Olig2 in adult uninjured mice (Fig. 10biii), significantly decreasing after optic nerve crush to 31.0% ± 3.8% at 10 days pONC ($P = 0.0205$; Fig. 10ciii) and further to 3.0% ± 3.7% at 6 weeks pONC ($P = 0.0012$; Fig. 10diii). The decrease in Olig2 was statistically significant between the two injured groups ($P = 0.0008$).

Discussion

Here we present a systemic analysis of developmentally important guidance cues in the embryonic, adult uninjured and adult injured visual pathway in mice. The findings are summarized in the Table.

In the developing embryo there is a specialized cellular arrangement at the optic chiasm midline, consisting of a palisade of radial glia cells that are positive for BLBP and RC2, which support growth of both crossed and uncrossed retinal neurites.[20,32,45,46] Similar results have been shown using embryonic tissue in this study, where a palisade of radial glia, also positive for RC2 and BLBP, were identified immediately above the optic chiasm midline with end feet that extend through the optic chiasm midline. Hartfuss and coworkers[53] showed that CNS RC2/GLAST/BLBP-positive radial astroglial cells lose the RC2 antigen during the postnatal period and that purified astrocytes in vitro are GLAST, BLBP, and GFAP positive but not RC2.[47,53,54] Thus, it was expected that mature astrocytes in the adult do not express RC2. However, in this study, $RC2^{+ve}/BLBP^{-ve}$ processes were observed in the adult optic chiasm midline area whereas the surrounding structures were devoid of the RC2 and BLBP positive palisade. These differences could be attributed to the differences between observations in vitro and in vivo. Interestingly when the adult optic nerve received a ONC injury, BLBP expression in glial processes within the chiasm was restored at the expense of RC2 10 days after this injury. Over a longer duration however both markers were absent. Ten days pONC, BLBP alone was also re-expressed in the area immediately superior to the chiasm. BLBP-positive astrocytes are found to accumulate in MS lesions, and it has been suggested that BLBP expression might aid tissue repair by promoting expression of several growth factors including FGF2, PDGF-AA and osteopontin.[55] In the context of the adult optic chiasm post injury, the appearance of BLBP-positive astroglia at an early stage postinjury may promote re-myelination and tissue repair processes, although further studies will be required to explore this relationship.

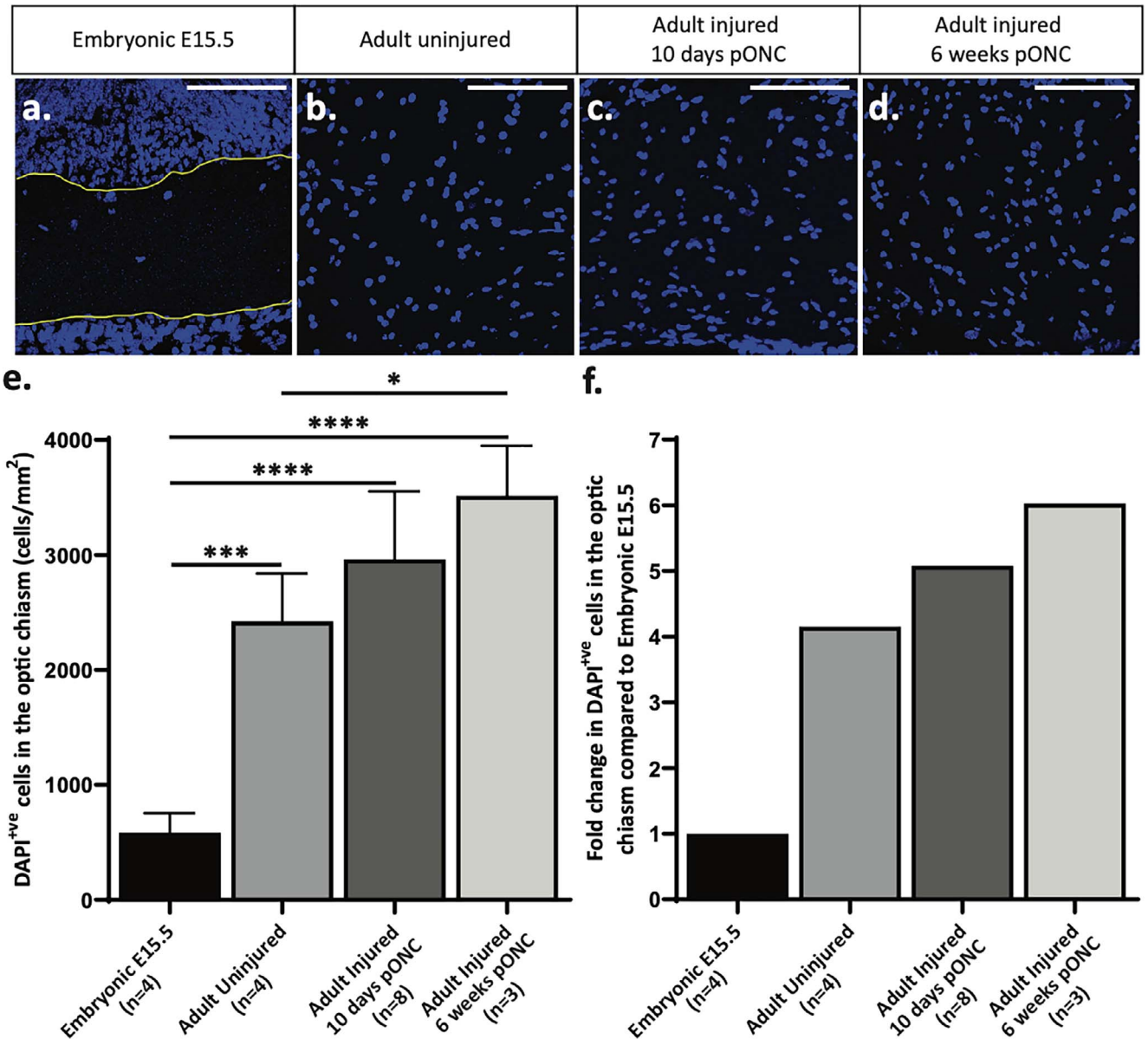

Figure 8. Quantification of DAPI-positive cells in the optic chiasm at E15.5 and in adult–uninjured and adult–injured samples. Images of the optic chiasm are shown at E15.5 in (**a**), with the optic chiasm outline in *yellow*, in adult uninjured tissue in (**b**), in adult injured tissue at 10 days pONC in (**c**) and in adult injured tissue at 6 weeks pONC in (**d**). The number of DAPI-positive cells in the optic chiasm were manually counted, with total numbers shown in (**e**) and fold-change in (**f**). *Blue*: DAPI. *Scale bar*: 100 µm.

Slit1 signaling plays an important role in guiding RGC axons toward their targets in the brain during development by a chemorepellent action that prevents RGC axons from invading non-target tissues.[34–36,56] In *X. laevis* a targeted downregulation of *xslit1* expression just before optic tract development results in an axon guidance defects whereby RGC axons fail to navigate a caudal turn in the mid-diencephalon.[57] We observed Slit1 expression in the optic tracts at E15.5, which was absent in the uninjured adult. However, at 10 days pONC, Slit1 expression was found at the optic chiasm midline, the structures surrounding the chiasm and the opposing optic tract, all of which may signal as a "no go" areas to regenerating RGC axons that express the corresponding Robo2 receptor. On the other hand, this pattern was not observed 6 weeks pONC which may indicate that axons struggle to regenerate beyond the optic chiasm due to the lack of this chemorepellent cue.

The expression of the growth permissive guidance cue Pax2 is important in the formation of the chiasm region in the developing embryo. At E11, Pax2 guides the first axons from the optic stalk into the brain and a transverse band of Pax2-expressing neuroepithelium extends from side to side of the ventral forebrain.[16,17,58,59] A similar profile of Pax2 staining was identified in this study. At E11.5, a transverse Pax2-expressing corridor was identified crossing the forebrain. At E15.5 Pax2 expression is confined to the junction between the optic nerves and optic chiasm. Here, for the first time we can show that in the adult mouse Pax2 expression remains confined to the optic nerve, stopping in the area where the optic nerve meets the chiasm, similar to that observed in the E15.5 embryo. Interestingly, Pax2 expression can be observed within the optic chiasm 10 days following a ONC but not 6 weeks after injury. It is unclear what impact Pax2 expression in this region has on regenerating RGC axons. Pax2 is a

Investigative Ophthalmology & Visual Science

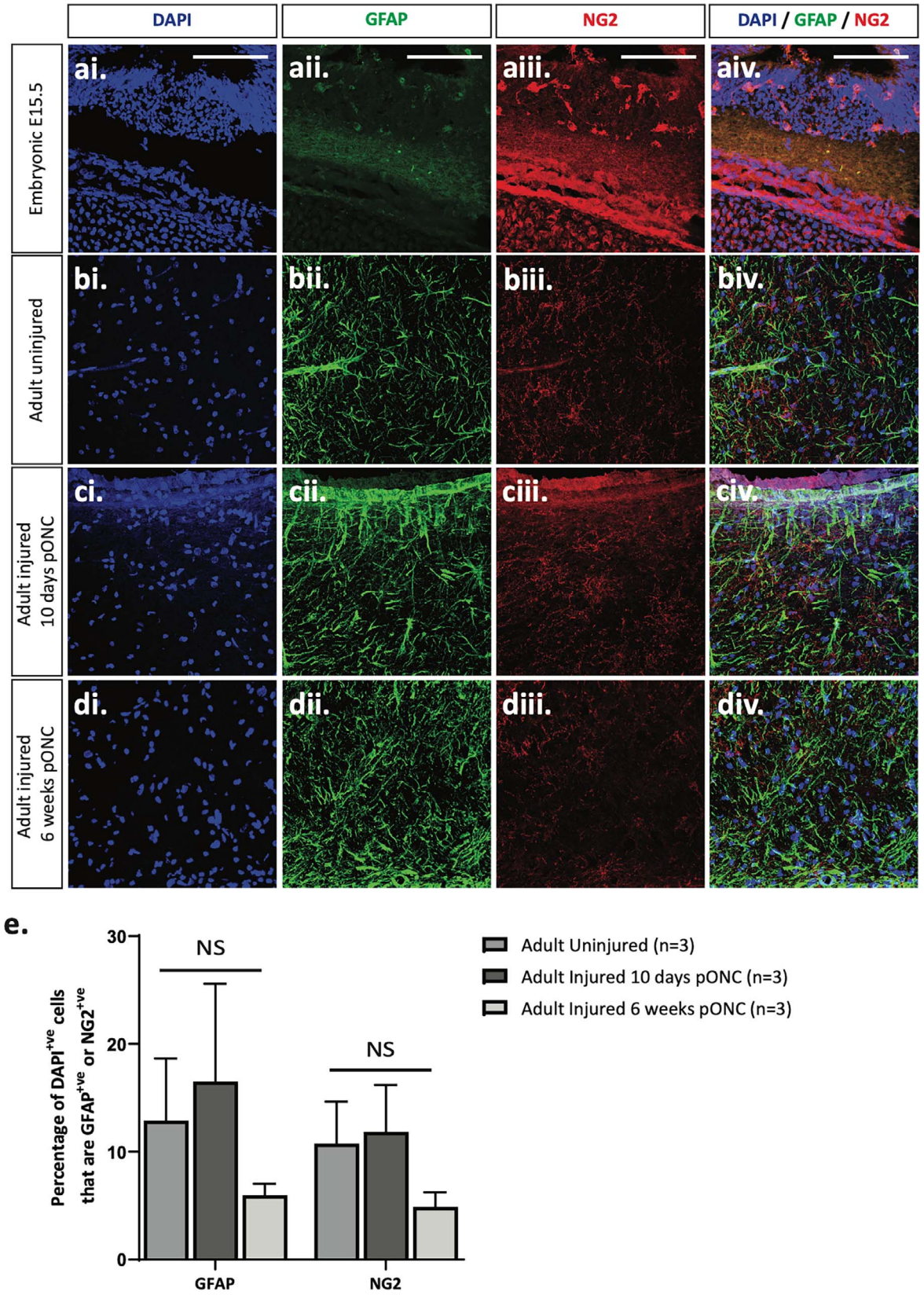

Figure 9. GFAP (*green*) and NG2 (*red*) labeling in the optic chiasm at E15.5 and in adult uninjured and adult injured mouse coronal samples. Images of the optic chiasm at E15.5 are shown in (**ai–aiv**), in adult uninjured tissue in panel (**bi–biv**) and in adult injured tissue at 10 days pONC in (**ci–civ**) and at 6 weeks pONC in (**di–div**). GFAP (*green*) staining is shown in (**aii**, **bii**, **cii**, **dii**) and NG2 (*red*) staining is shown in (**aiii**, **biii**, **ciii**, **diii**). *Blue*: DAPI. *Scale bar*: 100 µm. The percentage of DAPI-positive cells colocalized with GFAP or NG2 in the optic chiasm in the adult uninjured compared to the adult injured samples was quantified and can be seen in the graph in (**e**).

Investigative Ophthalmology & Visual Science

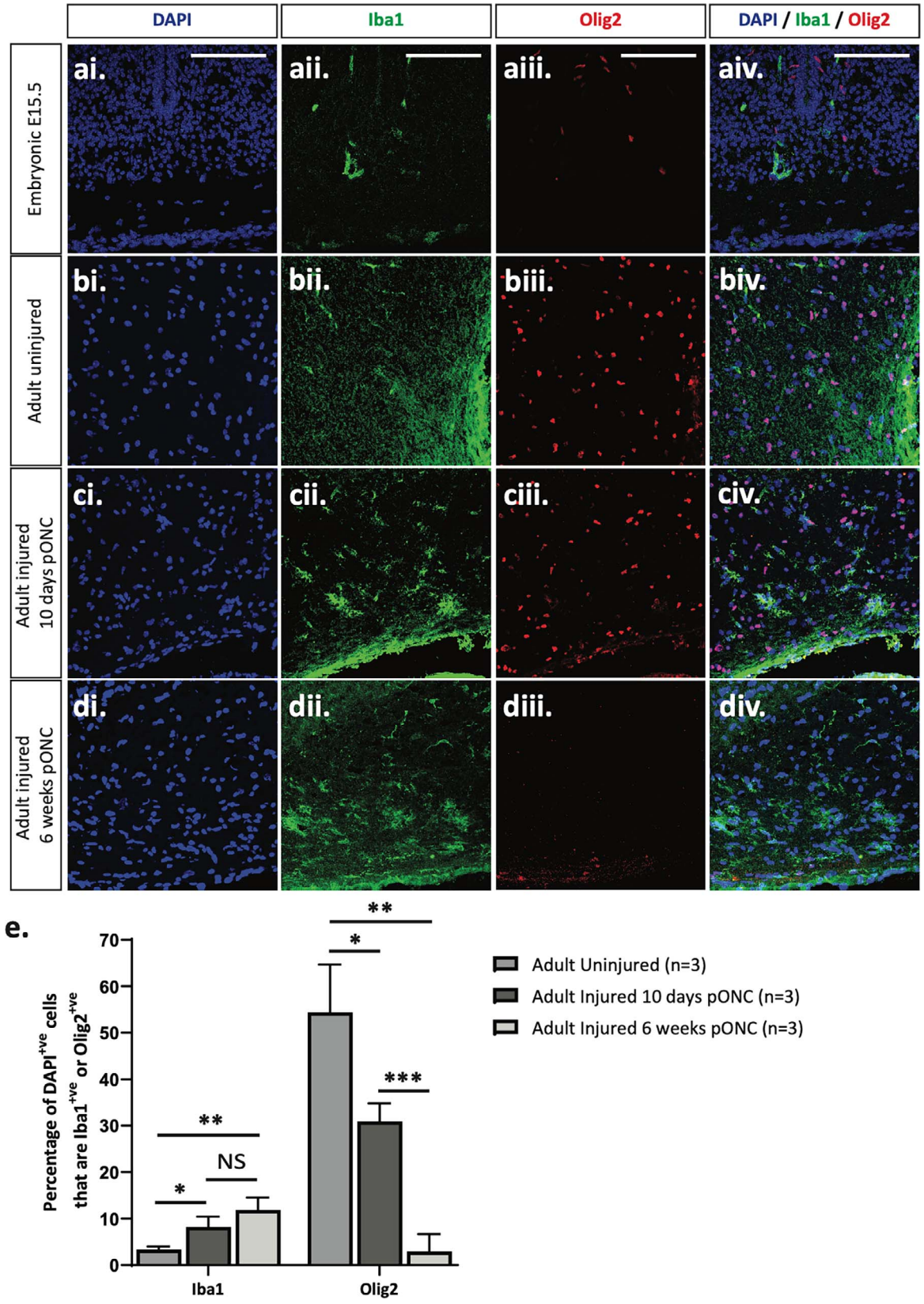

Figure 10. Iba1 (*green*) and Olig2 (*red*) labelling in the optic chiasm at E15.5 and in adult uninjured and adult injured mouse coronal samples. Images of the optic chiasm at E15.5 are shown in (**ai–aiv**), in adult uninjured tissue in (**bi–biv**) and in adult injured tissue at 10 days pONC in (**ci–civ**) and at 6 weeks pONC in (**di–div**). Iba1 (*green*) staining is shown in (**aii**, **bii**, **cii**, **dii**) and Olig2 (*red*) staining is shown in (**aiii**, **biii**, **ciii**, **diii**). *Blue*: DAPI. *Scale bar*: 100 μm. The percentage of DAPI-positive cells colocalized with Iba1 or Olig2 in the optic chiasm in the adult uninjured compared to the adult injured samples was quantified and can be seen in the graph in panel **e**.

Investigative Ophthalmology & Visual Science

Table. Guidance Cues Summary

Markers	Location	Embryonic	Adult Uninjured	Adult, 10 Days pONC	Adult, 6 Weeks pONC
RC2 & BLBP	Superior to the optic chiasm	RC2+/BLBP+	RC2−/BLBP−	RC2−/BLBP+	RC2−/BLBP−
	Processes in the chiasm midline	RC2+/BLBP+	RC2+/BLBP−	RC2−/BLBP+	RC2−/BLBP−
Slit1	Superior to the optic chiasm	Slit1−	Slit1−	Slit1+	Slit1−
	Optic chiasm midline	Slit1−	Slit1−	Slit1+	Slit1−
	Optic tracts	Slit1+	Slit1−	Slit1+ opposing optic tract	Slit1−
Pax2	Optic chiasm midline	Pax2−	Pax2−	Pax2+	Pax2−
	Junction between the optic chiasm and optic nerves junction	Pax2+	Pax2+	Pax2+	Pax2−
CSPGs	Superior to the optic chiasm	CSPGs+	CSPGs−	CSPGs−	CSPGs−
	Junction between the optic chiasm and optic tracts	CSPGs+	CSPGs−	CSPGs−	CSPGs−

transcription factor whose expression is controlled by FGF8 and Wnt1 during development, and loss/gain of function developmental studies indicate that Pax2 is responsible for appropriate RGC axons guidance throughout the optic nerve and chiasm.[15,16,43] More specifically it is thought that Pax2 regulates the expression of surface molecules, CD44 and L1, involved in contact attraction.[60] Studies using the goldfish, a species capable of regenerating RGC axons, indicated a causal role for Pax2 in regeneration. Parrilla et al.[40] demonstrated that there is a Pax2+ astrocyte population, which increases in the optic nerve head during the regeneration period of RGC axons, although the exact function of this cell population remains to be investigated.

Together with Slit1, CSPGs expression is important during development and it has been shown to create a chemo-repellent boundary that avoids non-target invasion by developing axons while travelling in the brain.[37,38,50] In this study, it is shown that in E15.5 brain samples, CS-56 was observed at the junction between the optic chiasm and optic tract, as well as the region immediately superior to the optic chiasm. Interestingly, both 2H6 and CS-56 staining was absent in uninjured and ONC injured adult brain samples (both 10 days and 6 weeks pONC). To better understand the role of CSPG's in axonal guidance, further research would be required, and a more thorough understanding of which core proteins are expressed both temporally and regionally in the brain and their roles.

The number of DAPI-positive cells in the optic chiasm increased between embryonic stage E15.5 and adult mice, aged 6 to 8 weeks , likely due to brain maturation. In addition, there was a significant increase in the number of DAPI-positive cells between adult uninjured and adult injured samples at 6 weeks pONC, which could be due to cells being recruited to the chiasm following injury. To investigate this, markers for the four major glial populations found in the optic chiasm were assessed: oligodendrocyte precursor cells (NG2), astrocytes GFAP), mature oligodendrocytes (Olig2), and microglia (Iba1). On investigation of the cell types found in the chiasm, the percentage of DAPI-positive cells colocalized with Iba1 significantly increased between adult uninjured and adult injured samples. As microglia are the main form of active immune defense in the CNS and would be involved in phagocytosis of the dying axons and myelin following ONC injury, this is expected. The percentage of cells colocalized with Olig2 significantly decreased between the groups, indicating a reduction in the proportion of oligodendrocytes following injury. Oligodendrocytes are involved in myelination and these cells may decrease due to the axons from the injured optic nerve die. Their proportion may also decrease as that of injury-response cell types increases.

In conclusion, we demonstrate that there are key differences in guidance cue expression in the ONC injured adult optic chiasm and surrounding structures at different time points and when compared to the adult uninjured and embryonic visual system. The expression of certain guidance cues early after ONC injury in adult mice supports the transient growth responses observed immediately after injury and termed "abortive regeneration." The lack of guidance cue expression 6 weeks after ONC may explain why so few axons can correctly navigate the optic chiasm after a regeneration stimulus.[4,8–11,13] Further experiments in a paradigm of axon regeneration would help to understand the true importance of each one of these markers for regenerating axonal guidance into the brain, including the ability to modulate their expression. Taken together, we suggest these results are highly relevant when set in context with current RGC regeneration studies, which demonstrate erratic and inefficient RGC axon regeneration through the optic chiasm. The findings presented here may shed some light as to why regeneration of RGC axons through this region remains a significant challenge.

Acknowledgments

Supported by a Sir Henry Wellcome Post Doctoral Fellowship (ACB), the Cambridge Eye Trust, the Jukes Glaucoma Research Fund, Fight for Sight UK, King's College, and research in the laboratory is supported by core funding from Wellcome and MRC to the Wellcome-MRC Cambridge Stem Cell Institute.

Disclosure: **R. Conceição**, None; **R.S. Evans**, None; **C.S. Pearson**, None; **B. Hänzi**, None; **A. Osborne**, None; **S.S. Deshpande**, None; **K.R. Martin**, None; **A.C. Barber**, None

References

1. Yin Y, Cui Q, Li Y, et al. Macrophage-derived factors stimulate optic nerve regeneration. *J Neurosci*. 2003;23:2284–2293.
2. Müller A, Hauk TG, Fischer D. Astrocyte-derived CNTF switches mature RGCs to a regenerative state following inflammatory stimulation. *Brain*. 2007;130:3308–3320.
3. Li S, Yang C, Zhang L, et al. Promoting axon regeneration in the adult CNS by modulation of the melanopsin/GPCR signaling. *Proc Natl Acad Sci U S A.*. 2016;113:1937–1942.
4. Lim JH, Stafford BK, Nguyen PL, et al. Neural activity promotes long-distance, target-specific regeneration of adult retinal axons. *Nat Neurosci*. 2016;19:1073–1084.
5. Park KK, Liu K, Hu Y, et al. Promoting axon regeneration in the adult CNS by modulation of the PTEN/mTOR pathway. *Science*. 2008;322:963–966.
6. Leibinger M, Müller A, Andreadaki A, Hauk TG, Kirsch M, Fischer D. Neuroprotective and axon growth-promoting

effects following inflammatory stimulation on mature retinal ganglion cells in mice depend on ciliary neurotrophic factor and leukemia inhibitory factor. *J Neurosci*. 2009;29:14334–14341.

7. Smith PD, Sun F, Park KK, et al. SOCS3 deletion promotes optic nerve regeneration in vivo. *Neuron*. 2009;64:617–623.
8. Kurimoto T, Yin Y, Omura K, et al. Long-distance axon regeneration in the mature optic nerve: contributions of oncomodulin, cAMP, and pten gene deletion. *J Neurosci*. 2010;30:15654–15663.
9. de Lima S, Koriyama Y, Kurimoto T, et al. Full-length axon regeneration in the adult mouse optic nerve and partial recovery of simple visual behaviors. *Proc Natl Acad Sci U S A*. 2012;109:13465–13465.
10. Sun F, Park KK, Belin S, et al. Sustained axon regeneration induced by co-deletion of PTEN and SOCS3. *Nature*. 2012; 480:372–375.
11. Pernet V, Joly S, Dalkara D, et al. Long-distance axonal regeneration induced by CNTF gene transfer is impaired by axonal misguidance in the injured adult optic nerve. *Neurobiol Dis*. 2013;51:202–213.
12. Qin S, Zou Y, Zhang CL. Cross-talk between KLF4 and STAT3 regulates axon regeneration. *Nat Commun*. 2013;4:1–9.
13. Luo X, Salgueiro Y, Beckerman SR, Lemmon VP, Tsoulfas P, Park KK. Three-dimensional evaluation of retinal ganglion cell axon regeneration and pathfinding in whole mouse tissue after injury. *Exp Neurol*. 2013;247:653–662.
14. Pernet V, Schwab ME. Lost in the jungle: new hurdles for optic nerve axon regeneration. *Trends Neurosci*. 2014;37:381–387.
15. Thanos S, Püttmann S, Naskar R, Rose K, Langkamp-Flock M, Paulus W. Potential role of Pax-2 in retinal axon navigation through the chick optic nerve stalk and optic chiasm. *J Neurobiol*. 2004;59:8–23.
16. Torres M, Gómez-Pardo E, Gruss P. Pax2 contributes to inner ear patterning and optic nerve trajectory. *Development*. 1996;122:3381–3391.
17. Alvarez-Bolado G, Schwarz M, Gruss P. Pax-2 in the chiasm. *Cell Tissue Res*. 1997;290:197–200.
18. Trousse F, Martí E, Gruss P, Torres M, Bovolenta P. Control of retinal ganglion cell axon growth: a new role for Sonic hedgehog. *Development*. 2001;128:3927–3936.
19. Plump AS, Erskine L, Sabatier C, et al. Slit1 and Slit2 cooperate to prevent premature midline crossing of retinal axons in the mouse visual system. *Neuron*. 2002;33:219–232.
20. Williams SE, Mann F, Erskine L, et al. Ephrin-B2 and EphB1 mediate retinal axon divergence at the optic chiasm. *Neuron*. 2003;39:919–935.
21. Hao Y, Wang J, Chan C-K, Chan S-O. Disruption of Sonic hedgehog signaling affects axon routing in the mouse optic chiasm. *Neuroembryology Aging*. 2006;4:76–84.
22. Sakai JA. Semaphorin 3d guides laterality of retinal ganglion cell projections in zebrafish. *Development*. 2006;133:1035–1044.
23. Sanchez-Camacho C, Bovolenta P. Autonomous and non-autonomous Shh signalling mediate the in vivo growth and guidance of mouse retinal ganglion cell axons. *Development*. 2008;135:3531–3541.
24. Dell AL, Fried-Cassorla E, Xu H, Raper JA. cAMP-induced expression of neuropilin1 promotes retinal axon crossing in the zebrafish optic chiasm. *J Neurosci*. 2013;33:11076–11088.
25. Erskine L, Herrera E. Connecting the retina to the brain. *ASN Neuro*. 2014;6:1759091414456210.
26. Wit J, Verhaagen J. Semaphorins: receptor and intracellular signaling mechanisms. *Adv Exp Med Biol*. 2007;600:24–32.
27. Yan-Li H, Sun-on C, Wei-ren D. Changes of retinofugal pathway development in mouse embryos after sonic hedgehog antibody perturbation. *J South Med Univ*. 2006;26:1679–1684.
28. Marcus RC, Mason CA. The first retinal axon growth in the mouse optic chiasm: axon patterning and the cellular environment. *J Neurosci*. 1995;15:6389–6402.
29. Pratt T, Conway CD, Tian NM, Price DJ, Mason JO. Heparan sulphation patterns generated by specific heparan sulfotransferase enzymes direct distinct aspects of retinal axon guidance at the optic chiasm. *J Neurosci*. 2006;26:6911–6923.
30. Oster SF, Bodeker MO, He F, Sretavan DW. Invariant Sema5A inhibition serves an ensheathing function during optic nerve development. *Development*. 2003;130:775–784.
31. Kuwajima T, Yoshida Y, Takegahara N, et al. Optic chiasm presentation of semaphorin6d in the context of plexin-A1 and Nr-CAM promotes retinal axon midline crossing. *Neuron*. 2012;74:676–690.
32. Marcus RC, Blazeski R, Godement P, Mason CA. Retinal axon divergence in the optic chiasm: uncrossed axons diverge from crossed axons within a midline glial specialization. *J Neurosci*. 1995;15:3716–29.
33. Marcus RC, Shimamura K, Sretavan D, Lai E, Rubenstein JL, Mason CA. Domains of regulatory gene expression and the developing optic chiasm: Correspondence with retinal axon paths and candidate signaling cells. *J Comp Neurol*. 1999;403: 346–358.
34. Erskine L, Williams SE, Brose K. Retinal ganglion cell axon guidance in the mouse optic chiasm: expression and function of robos and slits. *J Neurosci*. 2000;20:4975–4982.
35. Niclou SP, Jia L, Raper JA. Slit2 is a repellent for retinal ganglion cell axons. *J Neurosci*. 2000;20:4962–4974.
36. Ringstedt T, Braisted JE, Brose K, et al. Slit inhibition of retinal axon growth and its role in retinal axon pathfinding and innervation patterns in the diencephalon. *J Neurosci*. 2000; 20:4983–4991.
37. Chung KY, Taylor JS, Shum DK, Chan SO. Axon routing at the optic chiasm after enzymatic removal of chondroitin sulfate in mouse embryos. *Development*. 2000;127:2673–2683.
38. Ichijo H, Kawabata I. Roles of the telencephalic cells and their chondroitin sulfate proteoglycans in delimiting an anterior border of the retinal pathway. *J Neurosci*. 2001;21:9304–9314.
39. Mi H, Barres BA. Purification and characterization of astrocyte precursor cells in the developing rat optic nerve. *J Neurosci*. 1999;19:1049–1061.
40. Parrilla M, Lillo C, Herrero-Turrion MJ, et al. Pax2 in the optic nerve of the goldfish, a model of continuous growth. *Brain Res*. 2009;1255:75–88.
41. Boije H, Ring H, López-Gallardo M, Prada C, Hallböök F. Pax2 is expressed in a subpopulation of Müller cells in the central chick retina. *Dev Dyn*. 2010;239:1858–1866.
42. Stanke J, Moose HE, El-Hodiri HM, Fischer AJ. Comparative study of Pax2 expression in glial cells in the retina and optic nerve of birds and mammals. *J Comp Neurol*. 2010;518:2316–2333.
43. Macdonald R, Scholes J, Strähle U, et al. The Pax protein Noi is required for commissural axon pathway formation in the rostral forebrain. *Development*. 1997;124:2397–2408.
44. Fabre PJ, Shimogori T, Charron F. Segregation of ipsilateral retinal ganglion cell axons at the optic chiasm requires the Shh receptor Boc. *J Neurosci*. 2010;30:266–275.
45. Davenport RW, Thies E, Nelson PG. Cellular localization of guidance cues in the establishment of retinotectal topography. *J Neurosci*. 1996;16:2074–2085.
46. Mason CA, Sretavan DW. Glia, neurons, and axon pathfinding during optic chiasm development. *Curr Opin Neurobiol*. 1997;7:647–653.

47. Misson JP, Edwards MA, Yamamoto M, Caviness VS. Identification of radial glial cells within the developing murine central nervous system: studies based upon a new immunohistochemical marker. *Dev Brain Res*. 1988;44:95–108.
48. Yamamoto Y, Atoji Y, Oohira A, Suzuki Y. Immunohistochemical localization of chondroitin sulfate in the forestomach of the sheep. *Eur J Histochem*. 1995;39:265–272.
49. Ichijo H, Kawabata I. Roles of the telencephalic cells and their chondroitin sulfate proteoglycans in delimiting an anterior border of the retinal pathway. *J Neurosci*. 2001;21:9304–9314.
50. Leung K-M, Taylor JS, Chan S-O. Enzymatic removal of chondroitin sulphates abolishes the age-related axon order in the optic tract of mouse embryos. *Eur J Neurosci*. 2003;17:1755–1767.
51. Osborne A, Khatib TZ, Songra L, et al. Neuroprotection of retinal ganglion cells by a novel gene therapy construct that achieves sustained enhancement of brain-derived neurotrophic factor/tropomyosin-related kinase receptor-B signaling. *Cell Death Dis*. 2018;9:1007.
52. Chung KY, Shum D, Chan S. Expression of chondroitin sulfate proteoglycans in the chiasm of mouse embryos. *J Comp Neurol*. 2000;417:153–163.
53. Hartfuss E, Galli R, Heins N, Götz M. Characterization of CNS precursor subtypes and radial glia. *Dev Biol*. 2001;229:15–30.
54. Edwards MA, Yamamoto M, Caviness VS. Organization of radial glia and related cells in the developing murine CNS. An analysis based upon a new monoclonal antibody marker. *Neuroscience*. 1990;36:121–144.
55. Kipp M, Gingele S, Pott F, et al. BLBP-expression in astrocytes during experimental demyelination and in human multiple sclerosis lesions. *Brain Behav Immun*. 2011;25:1554–1568.
56. Thompson H, Barker D, Camand O, Erskine L. Slits contribute to the guidance of retinal ganglion cell axons in the mammalian optic tract. *Dev Biol*. 2006;296:476–484.
57. Atkinson-Leadbeater K, Bertolesi GE, Hehr CL, Webber CA, Cechmanek PB, McFarlane S. Dynamic expression of axon guidance cues required for optic tract development is controlled by fibroblast growth factor signaling. *J Neurosci*. 2010;30:685–693.
58. Fotaki V, Price DJ, Mason JO. Newly identified patterns of Pax2 expression in the developing mouse forebrain. *BMC Dev Biol*. 2008;8:79.
59. Goode DK, Elgar G. The PAX258 gene subfamily: a comparative perspective. *Dev Dyn*. 2009;238:2951–2974.
60. Sretavan DW, Feng L, Pure E, Reichardt LF. Embryonic neurons of the developing optic chiasm express L1 and CD44, cell surface molecules with opposing effects on retinal axon growth. *Neuron*. 1994;12:957–975.

Investigative Ophthalmology & Visual Science